

Investigation of X-ray radiation response to electrical properties of Mo/Cu(In_{0.7}Ga_{0.3})Te₂/p-Si/Al semiconductor diode

Semih Ağca¹ , Semra Arslan² , Güven Çankaya³

Keywords:

*Semiconductor diode,
Chalcopyrite,
X-ray radiation,
Barrier height,
Series resistance*

Abstract — Diodes are exposed to radiation in many operating environments, and it is important to investigate the radiation effect. In this study, the impact of X-ray radiation on the electrical properties of Mo/Cu(In_{0.7}Ga_{0.3})Te₂/p-Si/Al semiconductor diode was explored by I-V measurements performed before and after radiation doses between 200 and 1000 centiGray. The semiconductor diode was exposed to radiation by a linear accelerator having 6 MV X-ray. I-V measurements and the Cheung-Cheung method demonstrated the differences in series resistance, ideality factor, and barrier height. Moreover, the interface state density was obtained from I-V results. The radiation dose increased the ideality factor and decreased the barrier height. This result was thought to be due to the increase in the interface state density and the defects in the diode interface. The series resistance was increased by increasing the radiation dose due to a possible decrease in mobility and free carrier concentration. As a result of exposure to X-ray, defects occurred and due to these defects, the diode deviated from the ideal. It has been observed that the electrical properties of the diode were sensitive to X-ray radiation. The study demonstrated that the Mo/Cu(In_{0.7}Ga_{0.3})Te₂/p-Si/Al semiconductor diode can be implemented in X-ray radiation detection systems.

Subject Classification (2020): 83C30, 35Q20

1. Introduction

Radiation detectors were needed in many fields such as medical diagnostic imaging and therapy, space and aviation, homeland security, and astrophysics [1,2]. The production of such detectors basically relies on semiconductor devices. Diode-based radiation sensors, photodiode-based radiation sensors, radiation-sensitive metal-oxide-semiconductor field-effect transistor (MOSFET) devices, static random-access memory (SRAM) based radiation monitor, built-in current sensor-based radiation detectors, memristor-based radiation sensors, and variable capacitor-based radiation sensors are some examples of radiation detectors [3]. Since radiation-semiconductor interaction is very important in radiation detectors, there has been a significant increase in studies about the effect of radiation on semiconductor devices [4-6]. Candelori et al. have investigated the effect of radiation on thin oxide p-channel MOSFETs. They demonstrated that the drain leakage current increased after irradiation [7]. Belousov et al. have studied the radiation effects on charge-coupled devices. They confirmed that the response of the charge-coupled device to radiation was linear [8]. The effect of radiation on drain and source regions of a

¹semihagca@aybu.edu.tr (Corresponding Author); ²arslnsmr@gmail.com; ³erguvan@rocketmail.com

^{1,2,3}Department of Metallurgical and Materials Engineering, Faculty of Engineering and Natural Sciences, Ankara Yıldırım Beyazıt University, Ankara, Türkiye

Article History: Received: 18 Sep 2023 — Accepted: 09 Nov 2023 — Published: 31 Dec 2023

MOSFET with two different configurations was investigated by İlik et al. [9]. They found that the leakage current of the straight configuration was much higher than that of the reverse configuration.

In recent years, compound semiconductor radiation detectors have more preferred due to their features such as adjustable bandgap [10]. CdZnTe has attracted more attention due to its high average atomic number, suitable bandgap, and low leakage current properties [11-14]. Hossain et al. have incorporated Mg into the compound instead of Zn and studied room temperature X-ray and gamma-ray detector properties of CdMgTe. They achieved good detector properties with fewer defects due to a lower concentration of Te inclusions [2].

Chalcopyrite compounds in radiation detectors have also attracted interest due to tunable electrical and optical properties. Stowe et al. have investigated the LiGaSe₂ chalcopyrite for semiconductor radiation detection applications. They improved electrical and optical properties by reducing crystal defects via annealing the LiGaSe₂ in Li metal vapor [15]. Ning et al. [16] developed a Cu(In,Ga)Se₂ chalcopyrite-based energy-resolved X-ray detector. They studied the effect of different Ga concentrations and found that the optimum Ga concentration was achieved with a Ga/(Ga+In) (GGI) of about 0.3.

Although the electrical and optical properties of Cu(In,Ga)Te₂ compound have been studied [17-20], deeper research was needed about the effect of radiation on the electrical properties of this compound. In this study, we tried to demonstrate the suitability of this compound for use in radiation detectors by examining the effect of radiation on its electrical properties.

2. Materials and Methods

A one-side polished B-doped p-type (100) Si wafer with a thickness of about 400 μm was used as substrate. The substrate was cleaned by standard chemical cleaning procedure [21]. The polished side of the chemically cleaned Si substrate was coated with Al by a vacuum evaporation unit under 10⁻⁵ torr vacuum. Al-coated Si substrate was heat treated at 575 °C for 3 minutes to complete the ohmic contact. Cu(In_{0.7}Ga_{0.3})Te₂ ingot was produced with pure Cu, In, Ga, and Te elements in a sealed quartz ampoule, explained in detail elsewhere [22]. 250 nm thick Cu(In_{0.7}Ga_{0.3})Te₂ was deposited on B-doped side of Si wafer with the same vacuum evaporation unit. Mo rectifying contact was deposited by magnetron sputtering. Mo contact was formed using a mask during the deposition with a diameter of about 1 mm. After all these steps, Mo/Cu(In_{0.7}Ga_{0.3})Te₂/p-Si/Al semiconductor diode was obtained.

To understand the effect of radiation on the electrical properties of the diode, forward bias I-V features were measured by Keithley 2400 source meter at room temperature in the dark before irradiation and after application of 200, 400, 600, 800 and 1000 centiGray (cGy) radiation doses by a 6 MV X-ray radiation source linear accelerator. The electrical parameters of the diode, such as ideality factor (n), barrier height (Φ_B), and series resistance (R_S), were obtained by the I-V plot and Cheung-Cheung method [23], and the results of the two methods were compared.

3. Results and Discussion

The forward bias I-V characteristics of the diode before and after irradiation are shown by a semi-logarithmic plot in Figure 1.

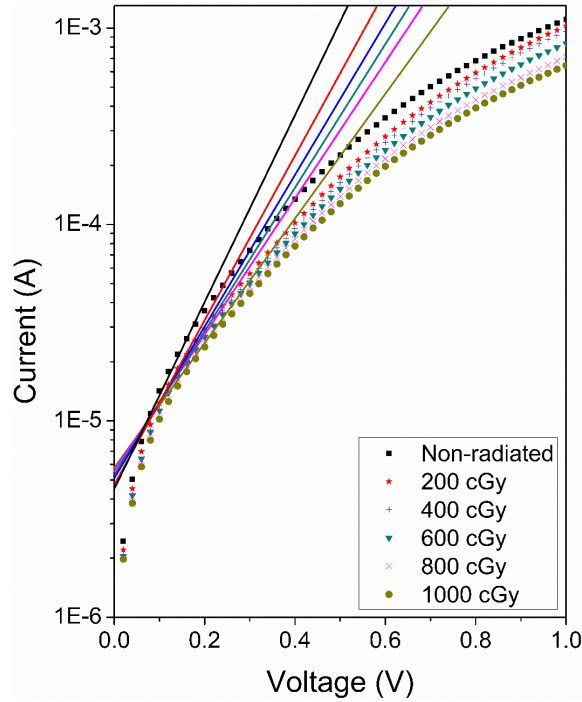


Figure 1. I-V graphs of the diode before and after X-ray exposure

The change in the graph with increasing radiation dose was found to be consistent with the literature [24]. The non-linear region at high forward bias values was due to the R_s which results from the contact wires or the bulk resistance of the semiconductor [25]. The non-linear I-V behavior of a typical diode was explained by the thermionic emission theory as follows [26,27]:

$$I = I_0 \exp\left(\frac{qV}{nkT}\right) \left[1 - \exp\left(-\frac{qV}{kT}\right)\right] \tag{3.1}$$

In (3.1), q , V , n , k , and T represent the electron charge, applied voltage, the ideality factor, Boltzmann’s constant, and the temperature in Kelvin, respectively. (3.1) can be rewritten for forward bias values larger than $3kT/q$ as,

$$I = I_0 \exp\left(\frac{qV}{nkT}\right) \tag{3.2}$$

The reverse saturation currents (I_0) were obtained from the interception of the linear portion of the semi-logarithmic I-V plot with the vertical axis by extrapolating to the zero bias and found to be 4.54×10^{-6} , 4.78×10^{-6} , 4.90×10^{-6} , 5.08×10^{-6} , 5.35×10^{-6} , 5.48×10^{-6} for non-radiated and 200, 400, 600, 800, and 1000 cGy radiated diode, respectively. The change in saturation current was comparable with similar studies in the literature [28,29]. I_0 can be expressed as,

$$I_0 = AA^*T^2 \exp\left(-\frac{q\Phi_B}{kT}\right) \tag{3.3}$$

In (3.3), A , A^* , and Φ_B represent the effective diode area, the effective Richardson constant which equals $32 \text{ A/cm}^2\text{K}^2$ for p-type Si, and the barrier height at zero bias, respectively. The ideality factor can be obtained from (3.2) as,

$$n = \frac{q}{kT} \left(\frac{dV}{d \ln I}\right)$$

The ideality factor, commonly used to determine the deviation of the diode from the ideal thermionic emission model, can be obtained from the slope of the linear region of the forward bias lnI-V plot. By using (3.3), the barrier height at zero bias can be expressed as,

$$\Phi_B = \frac{kT}{q} \ln\left(\frac{AA^*T^2}{I_0}\right) \tag{3.4}$$

Since the current curve in forward bias quickly becomes dominated by series resistance and deviates from linearity, the low forward bias parts of I-V characteristics were used to obtain the ideality factor. The forward bias lnI-V plots are shown in Figure 2.

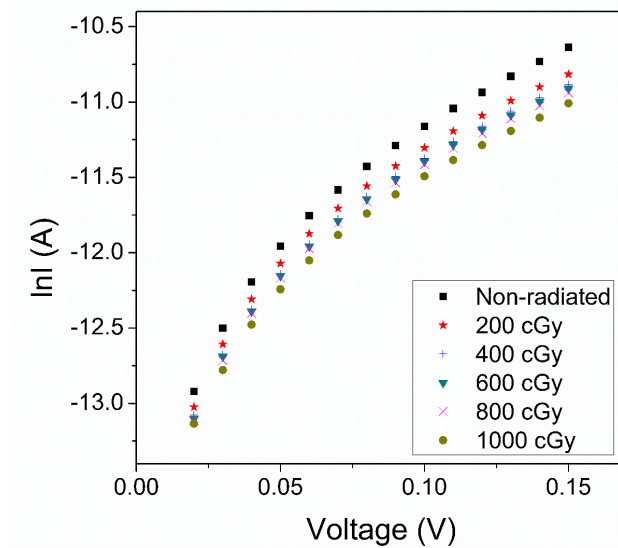


Figure 2. The forward bias lnI-V plots of the diode before and after irradiation

The barrier height was calculated by using (3.4). It should be noted that the barrier height is related to the potential barriers at the interfaces between p-Si, Cu(In_{0.7}Ga_{0.3})Te₂, and Mo. The barrier height and the ideality factor values of the diode obtained by I-V method are shown in Figure 3.

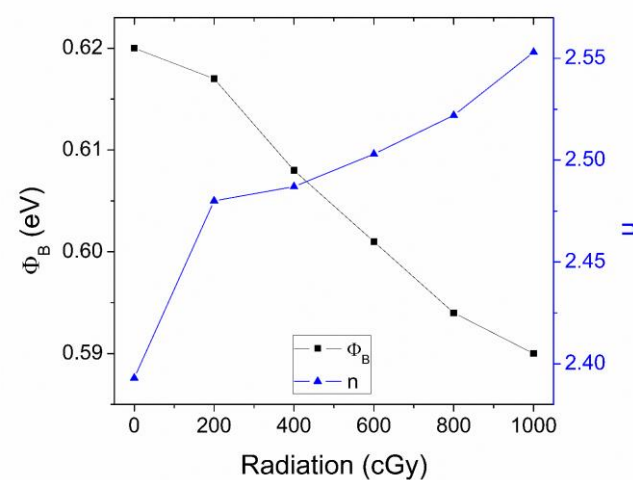


Figure 3. The barrier height and the ideality factor values of the diode obtained by I-V method

The relation between the applied radiation dose, the barrier height, and the ideality factor can be seen in Figure 3. As the radiation dose increased, the barrier height decreased, and the ideality factor increased. It was observed that the changes in barrier height and ideality factor were similar to the literature [30].

The series resistance, ideality factor, and barrier height were also obtained by the Cheung-Cheung method which can be expressed as follows:

$$\frac{dV}{d(\ln I)} = \frac{nkT}{q} + IR_s \tag{3.5}$$

$$H(I) = V - n\left(\frac{kT}{q}\right) \ln\left(\frac{I}{AA^*T^2}\right) \tag{3.6}$$

$$H(I) = IR_s + n\Phi_B \tag{3.7}$$

The ideality factor and the series resistance can be obtained by plotting the $dV/d\ln I$ versus I graphs which are shown in Figure 4.

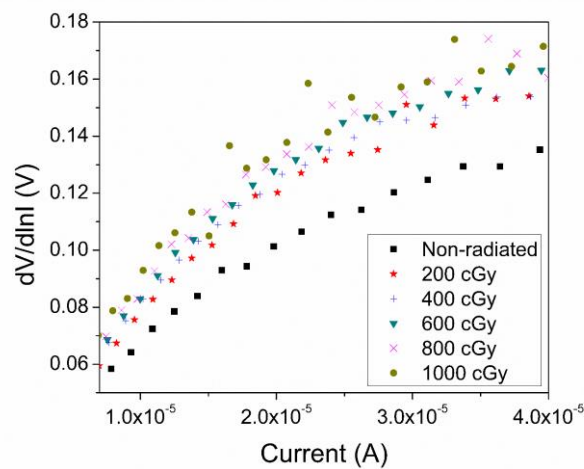


Figure 4. $dV/d\ln I$ versus I graphs of the diode before and after irradiation

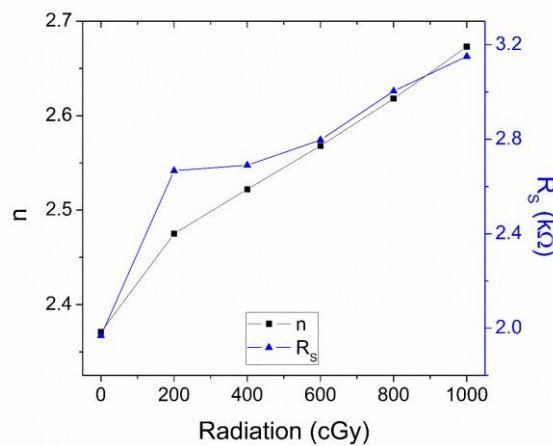


Figure 5. The ideality factor and series resistance values of the diode obtained by $dV/d\ln I$ vs I graphs. The best fits of $dV/d\ln I$ versus I graphs can be used to obtain the series resistance from the slope and the ideality factor from the vertical axis intercept according to (3.5). The ideality factor and the series resistance values of the diode obtained by $dV/d\ln I$ versus I graphs are shown in Figure 5.

It can be seen from Figure 5 that there is a linear relation between the ideality factor and the series resistance under the application of radiation with different doses. Both ideality factor and series resistance values increased with increasing radiation dose. The increase in the series resistance value with the increase in radiation dose was similar to both p-Si and other types of diodes in the literature [28,31].

The barrier height and the series resistance can also be obtained by using H(I) functions. H(I) versus I graphs of diode are shown in Figure 6.

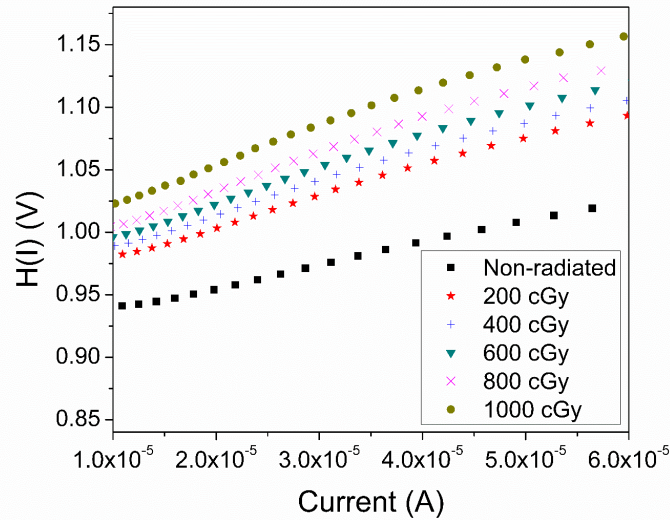


Figure 6. H(I) versus I graphs of the diode before and after irradiation

It can be obtained from (3.7) that the slope of H(I) versus I plot gives the series resistance, and the vertical axis intercept equals to $n\Phi_B$. Consequently, the barrier height can be calculated by using the ideality factor obtained from $dV/d\ln I$ versus I graph. The barrier height and the series resistance values of the diode obtained by H(I) versus I graphs are shown in Figure 7.

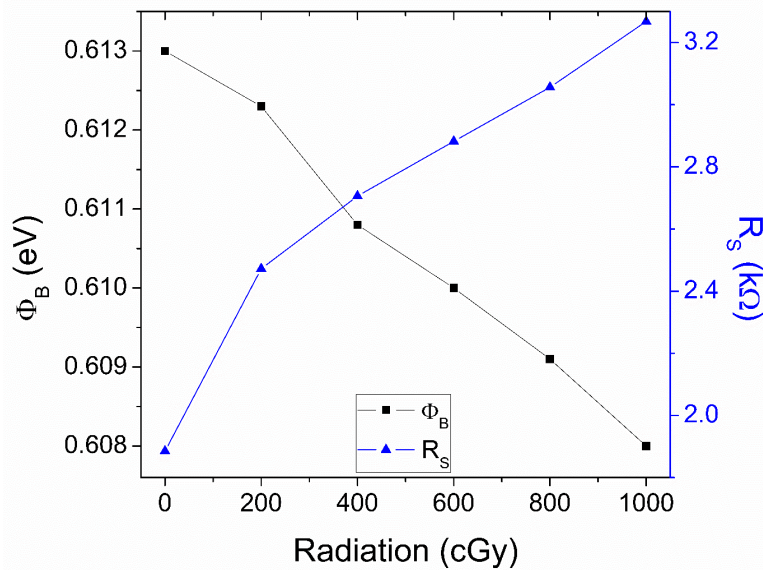


Figure 7. The barrier height and the series resistance values of the diode obtained by H(I) vs I graphs

The relation between the applied radiation dose, the barrier height, and the series resistance can be seen in Figure 7. As the radiation dose increased, the barrier height decreased, and the series resistance increased. By comparing Figure 3 and Figure 7, it can be seen that the barrier height values of the diode obtained by I-V and Cheung-Cheung methods were in good agreement with each other. To be able to compare different results obtained by different methods, the reverse saturation current, the barrier height, the ideality factor, and the series resistance values of diode under different radiation doses are shown in Table 1.

Table 1. The reverse saturation current, the barrier height, the ideality factor, and the series resistance values of diode under different radiation doses derived from different methods

Radiation (cGy)	I-V method			Cheung-Cheung method			
	Semi-log I-V		lnI vs V	dV/dlnI vs I		H(I) vs I	
	I_0 (A)	Φ_B (eV)	n	n	R_s (k Ω)	Φ_B (eV)	R_s (k Ω)
0	4.54x10 ⁻⁶	0.620	2.393	2.371	1.968	0.613	1.885
200	4.78x10 ⁻⁶	0.617	2.480	2.475	2.667	0.612	2.472
400	4.90x10 ⁻⁶	0.608	2.487	2.522	2.690	0.611	2.706
600	5.08x10 ⁻⁶	0.601	2.503	2.568	2.797	0.610	2.882
800	5.35x10 ⁻⁶	0.594	2.522	2.618	3.004	0.609	3.056
1000	5.48x10 ⁻⁶	0.590	2.553	2.673	3.151	0.608	3.268

It can be seen from Table 1 that the ideality factor values derived from the Cheung-Cheung method were higher than those obtained by the I-V method between 400 and 1000 cGy radiation doses, and these values were very close to each other for non-radiated and 200 cGy radiated diode. The higher ideality factor, in compliance with the literature [27,32], obtained by the Cheung-Cheung method was due to the nonlinearity of the I-V characteristics and the series resistance. On the other hand, the barrier height values were not obtained from the slopes of the I-V plot. Thus, the barrier height values obtained by different methods were close to each other for different radiation doses. Increasing the series resistance by increasing the radiation dose was agreed with the literature [33]. The series resistance values obtained by different plots were also comparable.

4. Conclusion

The nonlinear region of the semi-logarithmic I-V plot at higher applied voltages demonstrated that the series resistance became critical at high voltages [34]. The series resistance effect caused the diode to deviate from the ideal thermionic emission theory. This deviation resulted in higher values of the ideality factor than unity while lowering the barrier height values by increasing the radiation dose [35]. The radiation exposure might have caused defects at the Mo/Cu(In_{0.7}Ga_{0.3})Te₂/p-Si/Al interface, which is the reason for the decrease in the barrier height of the semiconductor diode. Another reason for the high ideality factor and low barrier height was thought to be the higher density of interface states with increasing radiation dose [36]. Series resistance values of irradiated samples were higher than those of non-radiated samples, showing that the product of mobility and free carrier concentration has decreased. The decrease in mobility might be due to the incorporation of defect centers by radiation exposure, which act as scattering centers.

Furthermore, introducing the deep traps might decrease the carrier concentration [37,38]. In conclusion, different X-ray radiation doses affected the electrical properties of the diode in different magnitudes. In other words, this type of diode could detect the change in radiation by means of electrical measurements. This situation demonstrated that the Mo/Cu(In_{0.7}Ga_{0.3})Te₂/p-Si/Al semiconductor diode can be implemented into the X-ray radiation detection systems. Detailed deep defect characterization can be investigated for future studies to better understand the interaction between the radiation and the semiconductor diode.

Author Contributions

All the authors equally contributed to this work. This paper is derived from the second author's master's thesis supervised by the third author. They all read and approved the final version of the paper.

Conflict of Interest

All the authors declare no conflict of interest.

Acknowledgment

This work was supported by the Projects Office of Ankara Yıldırım Beyazıt University, Grant number: 599-3371.

References

- [1] E. Vittone, J. G. Lopez, M. Jaksic, M. C. J. Ramos, A. Lohstroh, Z. Pastuovic, S. Rath, R. Siegele, N. Skukan, G. Vizkelethy, A. Simon, *Determination of radiation hardness of silicon diodes*, Nuclear Instruments and Methods in Physics Research Section B: Beam Interactions with Materials and Atoms 449 (2019) 6–10.
- [2] A. Hossain, V. Yakimovich, A. E. Bolotnikov, K. Bolton, G. S. Camarda, Y. Cui, J. Franc, R. Gul, K. H. Kim, H. Pittman, G. Yang, R. Herpst, R. B. James, *Development of cadmium magnesium telluride (Cd_{1-x}Mg_xTe) for room temperature X- and gamma-ray detectors*, Journal of Crystal Growth 379 (2013) 34–40.
- [3] A. Karmakar, J. Wang, J. Prinzie, V. De Smedt, P. Leroux, *A review of semiconductor based ionizing radiation sensors used in harsh radiation environments and their applications*, Radiation 1 (3) (2021) 194–217.
- [4] M. A. Salari, E. Şenarşlan, B. Güzeldir, M. Sağlam, *Effects of the γ - radiation on the electrical characteristics of the Au/n-Si/Au-Sb Schottky diode*, Journal of Physics: Conference Series 707 (1) (2016) Article Number 012018 7 pages.
- [5] S. Priyadarshi, V. Dubey, S. Dubey, *Effect of various radiations on the working of P-N junction diode*, International Journal of Advanced Research in Electrical, Electronics and Instrumentation Engineering 6 (5) (2017) 4016–4023.
- [6] M. B. Tagaev, *Effect of ionizing radiation on the silicon IMPATT diode characteristics*, Turkish Journal of Physics 23 (6) (1999) 985–988.
- [7] A. Candelori, D. Contarato, N. Bacchetta, D. Bisello, G. Hall, E. Noah, M. Raymond, J. Wyss, *High-energy ion irradiation effects on thin oxide p-channel MOSFETs*, IEEE Transactions on Nuclear Science 49 (3) (2002) 1364–1371.
- [8] A. Belousov, E. Mustafin, W. Ensinger, *Short and long term ionizing radiation effects on charge-coupled devices in radiation environment of high-intensity heavy ion accelerators*, Journal of Instrumentation 7 (11) (2012) Article Number C11002 6 pages.
- [9] S. İlik, F. B. Gencer, N. Ş. Solmaz, A. Çağlar, M. B. Yelten, *Radiation tolerance impact of trap density near the drain and source regions of a MOSFET*, Nuclear Instruments and Methods in Physics Research Section B: Beam Interactions with Materials and Atoms 449 (2019) 1–5.
- [10] A. Owens, A. Peacock, *Compound semiconductor radiation detectors*, Nuclear Instruments and Methods in Physics Research Section A: Accelerators, Spectrometers, Detectors and Associated Equipment 531 (1-2) (2004) 18–37.
- [11] G. Yang, A. E. Bolotnikov, P. M. Fochuk, O. Kopach, J. Franc, E. Belas, K. H. Kim, G. S. Camarda, A. Hossain, Y. Cui, A. L. Adams, A. Radja, R. Pinder, R. B. James, *Post-growth thermal annealing study*

of CdZnTe for developing room-temperature X-ray and gamma-ray detectors, Journal of Crystal Growth 379 (2013) 16–20.

- [12] P. Fochuk, R. Grill, I. Nakonechnyi, O. Kopach, O. Panchuk, Y. Verzhak, E. Belas, A. E. Bolotnikov, G. Yang, R. B. James, *Effect of Cd_{0.9}Zn_{0.1}Te:In crystals annealing on their high-temperature electrical properties*, IEEE Transactions on Nuclear Science 58 (5) (2011) 2346–2351.
- [13] K. H. Kim, J. Suh, A. E. Bolotnikov, P. M. Fochuk, O. V. Kopach, G. S. Camarda, Y. Cui, A. Hossain, G. Yang, J. Hong, R. B. James, *Temperature-gradient annealing of CdZnTe under Te overpressure*, Journal of Crystal Growth 354 (1) (2012) 62–66.
- [14] Y. Gu, C. Rong, Y. Xu, H. Shen, G. Zha, N. Wang, H. Lv, X. Li, D. Wei, W. Jie, *Effects of Te inclusions on charge-carrier transport properties in CdZnTe radiation detectors*, Nuclear Instruments and Methods in Physics Research Section B: Beam Interactions with Materials and Atoms 343 (2015) 89–93.
- [15] A. C. Stowe, J. Woodward, E. Tupitsyn, E. Rowe, B. Wiggins, L. Matei, P. Bhattacharya, A. Burger, *Crystal growth in LiGaSe₂ for semiconductor radiation detection applications*, Journal of Crystal Growth 379 (2013) 111–114.
- [16] D. Ning, M. Hu, M. Ma, Z. Wang, Z. Wang, Q. Wen, B. Du, E. Wang, S. Hu, M. Chen, C. Yang, W. Li, *A novel energy-resolved radiation detector based on the optimized CIGS photoelectric absorption layer*, Journal of Power Sources 536 (2022) Article ID 231520 10 pages.
- [17] O. Aissaoui, L. Bechiri, S. Mehdaoui, N. Benslim, M. Benabdeslem, X. Portier, H. Lei, J. L. Doualan, G. Nouet, A. Otmani, *Study of flash evaporated CuIn_{1-x}Ga_xTe₂ (x = 0, 0.5 and 1) thin films*, Thin Solid Films 517 (7) (2009) 2171–2174.
- [18] S. Fiat, P. Koralli, E. Bacaksiz, K. P. Giannakopoulos, M. Kompitsas, D. E. Manolacos, G. Çankaya, *The influence of stoichiometry and annealing temperature on the properties of CuIn_{0.7}Ga_{0.3}Se₂ and CuIn_{0.7}Ga_{0.3}Te₂ thin films*, Thin Solid Films 545 (2013) 64–70.
- [19] A. Karatay, B. Küçüköz, G. Çankaya, A. Ates, A. Elmalı, *The effect of Se/Te ratio on transient absorption behavior and nonlinear absorption properties of CuIn_{0.7}Ga_{0.3}(Se_{1-x}Te_x)₂ (0 ≤ x ≤ 1) amorphous semiconductor thin films*, Optical Materials 73 (2017) 20–24.
- [20] S. Fiat, E. Bacaksiz, M. Kompitsas, G. Çankaya, *Temperature and tellurium (Te) dependence of electrical characterization and surface properties for a chalcopyrite structured Schottky barrier diode*, Journal of Alloys and Compounds 585 (2014) 178–184.
- [21] N. Basman, R. Uzun, R. Ozcakır, I. Erol, G. Cankaya, O. Uzun, *Effect of a new methacrylic monomer on diode parameters of Ag/p-Si Schottky contact*, Journal of Microelectronics, Electronic Components and Materials 46 (4) (2016) 190–196.
- [22] S. Fiat, İ. Polat, E. Bacaksiz, M. Kompitsas, G. Çankaya, *The influence of annealing temperature and tellurium (Te) on electrical and dielectrical properties of Al/p-CIGSeTe/Mo Schottky diodes*, Current Applied Physics 13 (6) (2013) 1112–1118.
- [23] S. K. Cheung, N. W. Cheung, *Extraction of Schottky diode parameters from forward current-voltage characteristics*, Applied Physics Letters 49 (2) (1986) 85–87.
- [24] A. Siddiqui, M. Usman, *Radiation tolerance comparison of silicon and 4H-SiC Schottky diodes*, Materials Science in Semiconductor Processing 135 (2021) Article Number 106085 6 pages.

- [25] M. H. Suhail, I. M. Ibrahim, Z. Ahmad, S. M. Abdullah, K. Sulaiman, *ITO/PEDOT:PSS/MEH:PPV/Alq3/LiF/Au as a Schottky diode*, International Journal of Application or Innovation in Engineering & Management 2 (1) (2013) 130–136.
- [26] K. Akkiliç, A. Türüt, G. Çankaya, T. Kiliçoğlu, *Correlation between barrier heights and ideality factors of Cd/n-Si and Cd/p-Si Schottky barrier diodes*, Solid State Communications 125 (10) (2003) 551–556.
- [27] S. Sönmezoğlu, S. Şenkul, R. Taş, G. Çankaya, M. Can, *Electrical and interface state density properties of polyaniline-poly-3-methyl thiophene blend/p-Si Schottky barrier diode*, Solid State Sciences 12 (5) (2010) 706–711.
- [28] A. Kaymaz, E. E. Baydilli, H. U. Tecimer, Ş. Altındal, Y. Azizian-Kalandaragh, *Evaluation of gamma-irradiation effects on the electrical properties of Al/(ZnO-PVA)/p-Si type Schottky diodes using current-voltage measurements*, Radiation Physics and Chemistry 183 (2021) Article Number 109430 9 pages.
- [29] S. Krishnan, G. Sanjeev, M. Pattabi, *Electron irradiation effects on the Schottky diode characteristics of p-Si*, Nuclear Instruments and Methods in Physics Research Section B: Beam Interactions with Materials and Atoms 266 (4) (2008) 621–624.
- [30] D. A. Oeba, J. O. Bodunrin, S. J. Moloi, *Electrical properties of 3 MeV proton irradiated silicon Schottky diodes*, Physica B: Physics of Condensed Matter 610 (2021) Article Number 412786 6 pages.
- [31] E. E. Kutluoğlu, E. Ö. Orhan, Ö. Bayram, S. B. Ocak, *Gamma-ray irradiation effects on capacitance and conductance of graphene-based Schottky diode*, Physica B: Physics of Condensed Matter 621 (2021) Article Number 413306 7 pages.
- [32] S. Sönmezoğlu, C. B. Durmuş, R. Taş, G. Çankaya, M. Can, *Fabrication and electrical characterization of pyrrole-aniline copolymer-based Schottky diodes*, Semiconductor Science and Technology 26 (5) (2011) Article Number 055011 6 pages.
- [33] H. M. J. Al-Ta'ii, V. Periasamy, Y. M. Amin, *Electronic properties of DNA-based Schottky barrier diodes in response to alpha particles*, Sensors 15 (5) (2015) 11836–11853.
- [34] G. Lioliou, X. Meng, J. S. Ng, A. M. Barnett, *Characterization of gallium arsenide X-ray mesa p-i-n photodiodes at room temperature*, Nuclear Instruments and Methods in Physics Research Section A: Accelerators, Spectrometers, Detectors and Associated Equipment 813 (2016) 1–9.
- [35] H. Çulcu, M. Gökçen, A. Allı, S. Allı, *Current-voltage characteristics of Au/PLiMMA/n-Si diode under ultraviolet irradiation*, Journal of Physics and Chemistry of Solids 103 (2017) 197–200.
- [36] S. Nigam, J. Kim, F. Ren, G. Y. Chung, M. F. MacMillan, R. Dwivedi, T. N. Fogarty, R. Wilkins, K. K. Allums, C. R. Abernathy, S. J. Pearton, J. R. Williams, *High energy proton irradiation effects on SiC Schottky rectifiers*, Applied Physics Letters 81 (13) (2002) 2385–2387.
- [37] S. Chand, J. Kumar, *Current-voltage characteristics and barrier parameters of Pd2Si/p-Si(111) Schottky diodes in a wide temperature range*, Semiconductor Science and Technology 10 (12) (1995) Article Number 1680 6 pages.
- [38] M. E. Stuckelberger, T. Nietzold, B. West, R. Farshchi, D. Poplavskyy, J. Bailey, B. Lai, J. M. Maser, M. I. Bertoni, *Defect activation and annihilation in CIGS solar cells: an operando x-ray microscopy study*, Journal of Physics: Energy 2 (2) (2020) Article Number 025001 13 pages.